



Migration and Localization of Metal Atoms on Strained Graphene

Ovidiu Cretu,¹ Arkady V. Krashenninnikov,^{2,3} Julio A. Rodríguez-Manzo,¹ Litao Sun,^{1,4}
Risto M. Nieminen,³ and Florian Banhart^{1,*}

¹*Institut de Physique et Chimie des Matériaux, UMR 7504 CNRS, Université de Strasbourg,
23 rue du Loess, 67034 Strasbourg, France*

²*Department of Physics, University of Helsinki, P.O. Box 43, FI-00014 Helsinki, Finland*

³*Department of Applied Physics, Aalto University, P.O. Box 1100, FI-00076 Aalto, Finland*

⁴*SEU-FEI Nano-Pico Center, Key Laboratory of MEMS of Ministry of Education, Southeast University,
Si-Pai-Lou 2, Nanjing 210096, China*

(Received 26 July 2010; published 5 November 2010)

Reconstructed point defects in graphene are created by electron irradiation and annealing. By applying electron microscopy and density functional theory, it is shown that the strain field around these defects reaches far into the unperturbed hexagonal network and that metal atoms have a high affinity to the nonperfect and strained regions of graphene. Metal atoms are attracted by reconstructed defects and bonded with energies of about 2 eV. The increased reactivity of the distorted π -electron system in strained graphene allows us to attach metal atoms and to tailor the properties of graphene.

DOI: 10.1103/PhysRevLett.105.196102

PACS numbers: 68.65.Pq, 68.37.Lp, 71.15.Mb, 71.15.Nc

Any device application of graphene [1,2] relies on our ability to tailor its electronic or magnetic properties. Several routes have been proposed, e.g., self-doping by lattice defects [2,3] or doping with surface layers [4] or weakly adsorbed molecular species [5]. It is an essential question how foreign species are attached to or incorporated in the graphene lattice. The π -electron system of graphene is modified when atoms or molecules are adsorbed on the surface, but these species are weakly attached to perfect graphene and migrate or evaporate. The other extreme would be substitutional impurities on lattice sites of graphene [6], but these are known to be strong electron scattering centers [2]. Here we suggest, as an alternative, the creation of reconstructed defects such as nonhexagonal rings [7,8]. These defects lead to a locally increased reactivity [9] and thus enable the formation of stable bonds with other atoms on the surface while preserving a coherent lattice. Attaching transition metal atoms with unfilled d orbitals does not only modify the electronic structure [6,10] but may also lead to collective phenomena such as ferromagnetism, Kondo effect, or spin density waves [11]. We study the interaction between defects in graphene and metal atoms by creating localization centers in graphene with an electron beam and observing the trapping of tungsten atoms. We find an attractive interaction between reconstructed defects in graphene [12] and metal atoms on the surface to a large lateral separation. The mechanism of attraction in a reconstructed two-dimensional lattice is different from the known mechanisms of point defect interaction in bulk systems and originates from an interplay of local strain around defects and electronic adsorption effects.

Graphene layers were produced by exfoliation from highly oriented pyrolytic graphite [13]. The samples were annealed at 900 °C in high vacuum where W atoms were

evaporated from a heated W filament onto the graphene layers. The graphene samples were mounted in a heating specimen stage of a transmission electron microscope (TEM, Jeol 2100F), operated at 100 and 200 kV. *In situ* observation of the behavior of W atoms was carried out in a temperature range 20 °C–650 °C at different beam current densities.

Because of their high mass, single W atoms and their migration can be monitored in real time in the TEM [14] where a time scale of approximately 0.3–300 s was accessible. Below 250 °C the graphitic lattice was progressively damaged by the 200 keV electrons, whereas above 250 °C the lattice remained coherent at all electron energies. When the microscope was first operated at 100 kV and a specimen temperature of 470 °C, isolated W atoms were seen on the graphene layers, but the W atoms were localized. At 200 kV, however, a migration of W atoms was observed in the whole temperature range. The W atoms remained stationary for typically 1–10 s until a sudden jump over a distance of 1–5 nm occurred. The jump lengths are different, but always much larger than interatomic distances. Hence, W atoms carry out a diffusional motion between distant sites. Figure 1 shows typical jumps of a W atom on a few-layer graphene sheet at 470 °C (movie M1 in the supplementary material [15]). After a certain time, most W atoms reach edges of graphene layers and get trapped there.

Both electron-beam intensity and specimen temperature have an influence on the jump frequency. Experiments below 500 °C and beam current densities in the range 40–270 A/cm² showed that displacements are induced mainly by the electron beam. At higher temperatures, thermal effects come into play. Below 250 °C, when the graphene lattice is heavily damaged by the beam, almost no jumps occur and the W atoms are pinned by larger

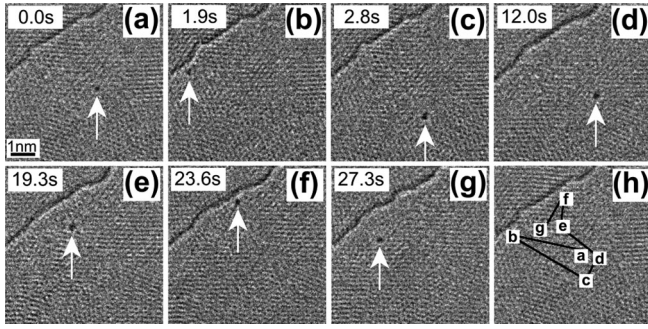


FIG. 1. Large-distance jumps of a W atom (arrowed) on a few-layer graphene sheet at 470 °C and an electron-beam current density of 110 A/cm². The total time [starting from (a)] is indicated. The whole path (a)–(g) is shown in (h). The dark line (top left) is the edge of a single graphene layer on the surface.

irradiation-induced lattice defects. In the range 250 °C–500 °C, the above-described jumping of W atoms is easily observable. Above 500 °C, however, the escape from the trapping centers seemed to be fast so that the highly mobile W atoms reach edges of graphene layers and get trapped within a short time (Fig. S2 in the supplementary material [15]). The observations of the W atoms were therefore concentrated on the intermediate temperature range (250 °C–500 °C).

During the hopping of the W atoms, an unexpected behavior was observed. The W atoms were often seen to

jump forth and back repeatedly between two sites having a distance of 0.5–1.4 nm. Figures 2(a)–2(d) show an example where a W atom oscillates between two positions (see movie M1 [15]). This shows that the W atoms do not execute a random walk; instead there seems to be an attraction between a W atom and a trapping site over a surprisingly long distance. When the W atoms were stationary between the large-distance jumps, a slight oscillation over a length of 1–3 Å occurred. Such a "vibration" of the atom around a localized trapping center is shown in Figs. 2(e)–2(g) (see movie M2 [15]). Short-distance jumps occur in the whole investigated temperature range (20 °C–650 °C), and their frequency is of the order 1 s^{−1}.

The observations show that W atoms are mobile on a graphene surface but can be trapped by defective sites. An escape from the trapping center can be induced thermally or by electron irradiation. Point defects can be produced by 200 keV electrons in graphenic structures [16], leaving vacancies where foreign species can be trapped [17]. Under the beam (200 keV, 100 A/cm²) each carbon atom can be displaced ballistically with a rate of 0.014 s^{−1}, assuming an average threshold displacement energy of 17 eV [18–20]. Thus, a certain concentration of single vacancies (SV) prevails, but divacancies (DV) [21] and 555-777 defects (three pentagons and three heptagons formed from a DV by bond rotation) [12] can also appear. At room temperature, DVs should dominate due to a higher

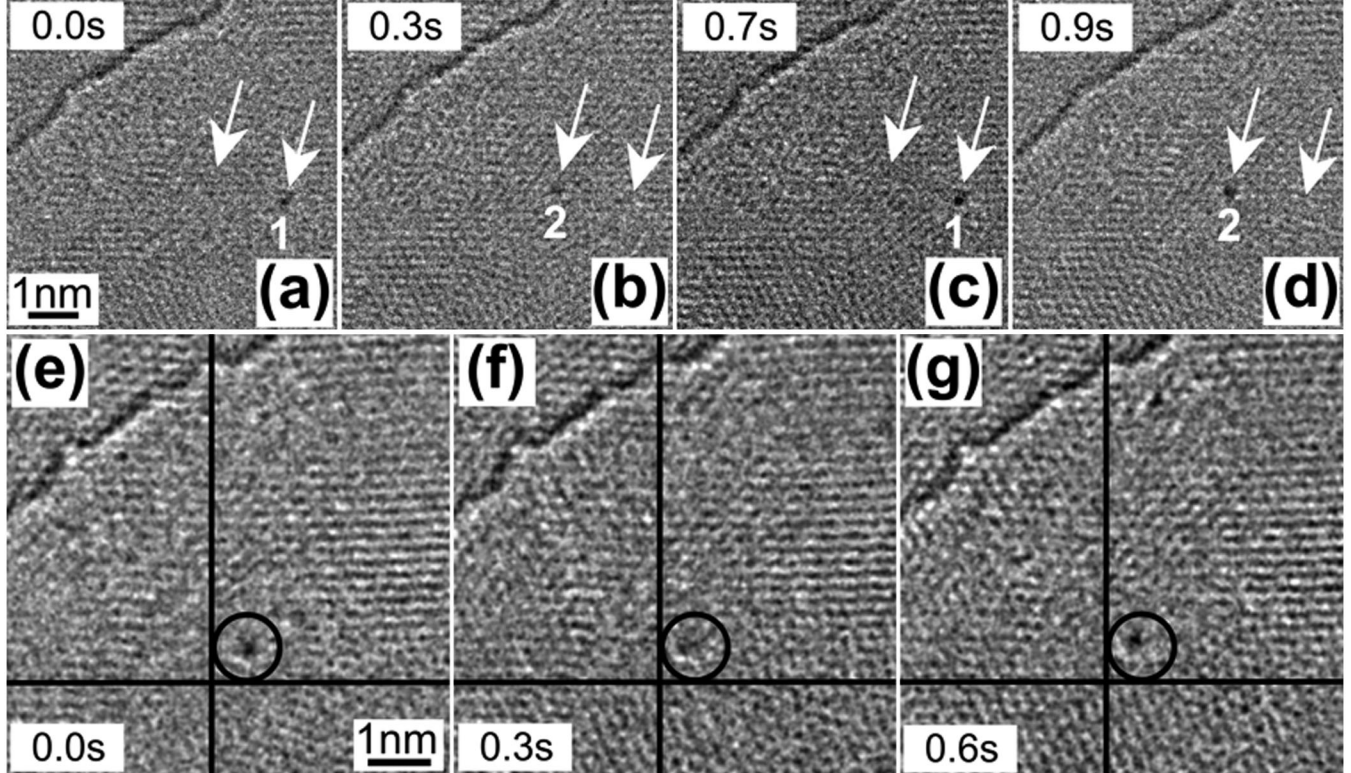


FIG. 2. Oscillations of a W atom on a few-layer graphene sheet at 480 °C. (a)–(d) Forth-and-back jumping between two distant trapping centers 1 and 2 (arrowed). (e)–(g) Small-scale oscillation around a trapping center. The circle is kept fixed on the lattice so that the migration of the W atom relative to the lattice is visible. The time scale is indicated.

displacement rate of carbon atoms at an undercoordinated SV [20], even when SVs are immobile. At elevated temperatures (over 200 °C), assuming a vacancy migration barrier of 1.2–1.3 eV, SVs coalesce to DVs [22], followed by transformations to 555-777 or similar defects [8,15], as this process lowers the total energy of the system by more than 1 eV per defect. Stone-Wales (55-77) defects can also appear under the electron beam, but their abundance is expected to be much lower than for vacancy-type defects, and bonding of adatoms to 55-77 defects is too weak to explain the experimental observations (Figs. S14 and S15 in [15]).

We carried out first-principles calculations by using spin-polarized density functional theory as implemented in the plane-wave-basis-set VASP [23] code (see Ref. [15] for details). We studied first the adsorption of a W atom onto a pristine graphene sheet [24] and found that the W atom may occupy stable positions above the middle of the hexagon (*H* position) and on top of a C-C carbon bond (bridge, or *B* position), the latter being lower in energy by 0.08 eV only. The adsorption energy is $E_a = -0.45$ eV in the *B* position, and the migration barrier of the W adatom is only of the order 0.1 eV. This does not allow stable trapping of W adatoms on perfect graphene at the temperatures of our experiment.

We found that W atoms bind strongly to the dangling bonds at SVs and DVs (−8.6 and −8.9 eV, respectively), similar to other transition metal atoms [6]. Such strong binding indicates that thermal detrapping at our experimental temperatures is not possible. As the 200 keV electrons can ballistically transfer no more than 2.8 eV to a W atom, irradiation-assisted depinning can also be excluded. Since W atoms were mobile in our experiments, we can hence exclude the existence of unreconstructed SVs and DVs in graphene above 250 °C.

The situation is different for the thermodynamically most stable 555-777 defect, as shown in Fig. 3(a). The adsorption energy of the W adatom on the defect is about 2 eV [Fig. 3(b)]. The drop in energy relative to the atom on perfect graphene results from the stretched carbon-carbon bonds at the defect where a higher electron density is available for forming new bonds with the adatom. A similar effect has earlier been reported for metal surfaces [25]. We found that here E_a is of the same order as the maximum transferred energy in a ballistic displacement. This means that depinning can occur in this experiment due to the beam effects at low temperatures. At elevated temperatures, thermally activated depinning is possible as well. If the difference between E_a on the defected and on pristine graphene is taken as a depth of the potential well (assuming the same jump frequency as for adatoms on pristine graphene), the rate would be of the order of 0.1 s^{-1} at 450 °C, in accordance with the experimental values. The adsorption energy $E_a \sim 2$ eV ensures stable trapping up to 200 °C.

We also calculated E_a for the W adatom in the vicinity of the 555-777 defect in various *B* or *H* positions [Fig. 3(a)], and the geometry was optimized without any constraints. We found that for all positions E_a is lower than that for the adatom on a pristine sheet, and that the energy decreases

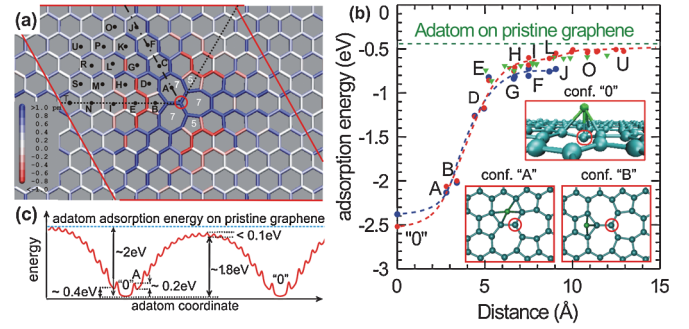


FIG. 3 (color). (a) Atomic structure of the 555-777 defect. The bonds are colored according to an increase (blue) or decrease (red) in the bond length (given in picometers). The bonds close to pentagons are contracted, but most C-C bonds are stretched. The letters indicate all nonequivalent positions of W adatoms in the *H* configurations. The red lines outline the (10×10) simulation cell. (b) Adsorption energy of a W adatom near the 555-777 defect as a function of separation between the adatom and the middle of the defect [circled atom in (a)]. The green triangles and red circles correspond to the bridge (*B*) and middle-of-hexagon (*H*) positions in the 10×10 unit cell. Blue dots stand for the *H* positions in the 7×7 supercell. The insets show the positions of the adatoms in the lowest energy configurations. (c) Energy of a W adatom in various positions on a graphene sheet with two 555-777 defects.

(i.e., bonding is stronger) when the adatom is closer to the defect. Thus, there is an increased bonding on strained hexagons around the defect, and the energy gradient may direct adatoms toward the 555-777 defects.

Several mechanisms may give rise to the gradient in E_a near the defect, the most obvious being (i) strain field-mediated interaction between the defect and adatom, (ii) interaction due to conduction electrons [26] related to Friedel oscillations near the defect, and (iii) direct Coulomb interaction between adatom and defect. Surprisingly, we found that none of them alone can explain the energy gradient. The 555-777 defect naturally gives rise to a strain field in its vicinity [Fig. 3(a)]. However, in a two-dimensional system the weakly bonded W adatom does not create a strain field of the opposite sign in the carbon network [15], and the conventional mechanism of vacancy-interstitial attraction as in 3D bulk systems does not work. Direct calculations of the charge density difference between the 555-777 defect and the pristine system showed that there is no charge redistribution nor charge density oscillations. The Coulomb interaction can be excluded as well, as there is no considerable charge transfer from the adatom and no localized charges on the adatom and defect.

To understand the nature of attractive interaction, we calculated E_a of W adatom on the strained graphene sheet. A biaxial strain of 1% (2%) lowers E_a for the *H* position from initially −0.38 to −0.54 (−0.69) eV, and for the *B* position from −0.45 to −0.52 (−0.59) eV, respectively. The drop in energy is associated with a smaller saturation of the C-C bonds under strain so that more electron density is available for making new bonds with the adatom. Thus,

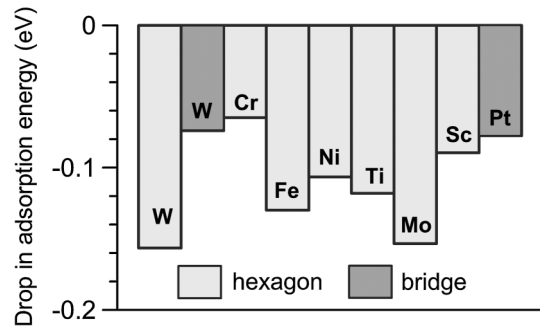


FIG. 4. Drop in the adsorption energy of metal adatoms adsorbed in the bridge and middle-of-hexagon positions on a nondefective graphene sheet under a biaxial strain of 1%. The energy drop is calculated with regard to the adsorption energy on unstrained graphene.

the observed energy gradient comes from a combination of the strain field and electronic effects. The range of attractive interaction should be 2–3 nm, in agreement with the experimental results.

The potential well for the adatom near the defect [Fig. 3(c)] can explain the attraction between the adatom and pinning centers, which is seen in TEM observations as a repeated jumping of the W atom between two trapping sites. The short-range jumps [Figs. 2(e)–2(g)] may be associated with the migration of the 555-777 defect itself. The defect can be transformed by bond rotation to a 5555-6-7777 defect [15], which is only 0.4 eV higher in energy. The barrier is, however, about 6 eV, as for the Stone-Wales transformation [27]. This value prohibits purely thermally induced migration, but as each carbon atom acquires such a kinetic energy every 6 s due to electron impacts, a combination of thermal and beam effects can explain the small oscillations.

This attraction mechanism should work for all adatoms that form covalent bonds with graphene. We calculated how the adsorption energy changes under a biaxial strain of 1% in the graphene layer. Figure 4 shows that E_a decreases with strain for all the elements we studied. The attractive interaction between the adatoms and defects is different from the known phenomenon of long-range interactions of adatoms on metals [28], graphite [29], or carbon nanotubes [30] which is mediated by purely electronic effects [31].

A detailed picture of the type and occurrence of defects in graphene has now been obtained by using W atoms as probes. It is apparent that the 555-777-type reconstructed vacancies are the predominant defect in a wide temperature range, and that they act as an efficient trapping center. The trapping of metal atoms in strained areas and at defects in graphene may be used for engineering the local electronic and magnetic structure of graphene, which is an alternative to substitutional doping. Once defects have been created, e.g., by irradiation or by a chemical treatment, metal atoms will find their way to the trapping center through the extended potential around each defect. If a pattern of defects is created, e.g., by electron-beam structuring [16,17], a migration of metal atoms along a predefined pathway could be stimulated.

Funding by the Agence Nationale de Recherche in France (NANOCONTACTS, NT09 507527) and the Ecole Doctorale de Physique in Strasbourg is gratefully acknowledged. L. S. acknowledges support from the National Basic Research Program of China (Grants No. 2009CB623702 and No. 2011CB707600), the National Natural Science Foundation of China (No. 60976003 and No. 51071044), and Open Research Fund of State Key Laboratory of Bioelectronics. This work was also supported by the Academy of Finland through several projects and the Centre of Excellence programme. We thank the Finnish IT Centre for Science for generous grants of computer time.

*Banhart@ipcms.u-strasbg.fr

- [1] A. K. Geim, *Science* **324**, 1530 (2009).
- [2] A. H. Castro Neto *et al.*, *Rev. Mod. Phys.* **81**, 109 (2009).
- [3] J. Lahiri *et al.*, *Nature Nanotech.* **5**, 326 (2010).
- [4] G. Giovannetti *et al.*, *Phys. Rev. Lett.* **101**, 026803 (2008).
- [5] T. O. Wehling *et al.*, *Nano Lett.* **8**, 173 (2008).
- [6] A. V. Krasheninnikov *et al.*, *Phys. Rev. Lett.* **102**, 126807 (2009).
- [7] A. J. Stone and D. J. Wales, *Chem. Phys. Lett.* **128**, 501 (1986).
- [8] J. C. Meyer *et al.*, *Nano Lett.* **8**, 3582 (2008).
- [9] S. M. Lee *et al.*, *Phys. Rev. Lett.* **82**, 217 (1999).
- [10] F. Banhart, *Nanoscale* **1**, 201 (2009).
- [11] B. Uchoa, C. Y. Lin, and A. H. Castro Neto, *Phys. Rev. B* **77**, 035420 (2008).
- [12] G. D. Lee *et al.*, *Phys. Rev. Lett.* **95**, 205501 (2005).
- [13] K. S. Novoselov *et al.*, *Science* **306**, 666 (2004).
- [14] N. Tanaka, H. Kimata, and T. Kizuka, *J. Electron Microsc.* **45**, 113 (1996).
- [15] See supplementary material at <http://link.aps.org/supplemental/10.1103/PhysRevLett.105.196102> for supplementary material and movies.
- [16] J. A. Rodriguez-Manzo and F. Banhart, *Nano Lett.* **9**, 2285 (2009).
- [17] J. A. Rodriguez-Manzo, O. Cretu, and F. Banhart, *ACS Nano* **4**, 3422 (2010).
- [18] A. V. Krasheninnikov and F. Banhart, *Nature Mater.* **6**, 723 (2007).
- [19] B. W. Smith and D. Luzzi, *J. Appl. Phys.* **90**, 3509 (2001).
- [20] A. V. Krasheninnikov *et al.*, *Phys. Rev. B* **72**, 125428 (2005).
- [21] A. A. El-Barbary *et al.*, *Phys. Rev. B* **68**, 144107 (2003).
- [22] A. V. Krasheninnikov *et al.*, *Chem. Phys. Lett.* **418**, 132 (2006).
- [23] G. Kresse and J. Furthmüller, *Comput. Mater. Sci.* **6**, 15 (1996).
- [24] P. Jensen, X. Blase, and P. Ordejón, *Surf. Sci.* **564**, 173 (2004).
- [25] M. Mavrikakis, B. Hammer, and J. K. Nørskov, *Phys. Rev. Lett.* **81**, 2819 (1998).
- [26] A. V. Shytov, D. A. Abanin, and L. S. Levitov, *Phys. Rev. Lett.* **103**, 016806 (2009).
- [27] L. Li, S. Reich, and J. Robertson, *Phys. Rev. B* **72**, 184109 (2005).
- [28] J. Repp *et al.*, *Phys. Rev. Lett.* **85**, 2981 (2000).
- [29] L. Hornekær, *Phys. Rev. Lett.* **96**, 156104 (2006).
- [30] G. Buchs *et al.*, *New J. Phys.* **9**, 275 (2007).
- [31] V. V. Cheianov and V. I. Falko, *Phys. Rev. Lett.* **97**, 226801 (2006).